Available online at www.sciencedirect.com
SCIENCE DIRECT®
Protein Expression and Purification 41 (2005) 384–392
Protein Expression & Purification
www.elsevier.com/locate/yprep

Characterisation of tyrosine-phosphorylation-defective calmodulin mutants

Valentina Salas[a,c,1], Juan Sánchez-Torres[a,1], David M. Cusidó-Hita[a], Yael García-Marchan[a,b,c], Felipe Sojo[c], Gustavo Benaim[b,c,*], Antonio Villalobo[a]

[a] *Instituto de Investigaciones Biomédicas, Consejo Superior de Investigaciones Científicas and Universidad Autónoma de Madrid, Arturo Duperier 4, E-28029 Madrid, Spain*
[b] *Centro de Biociencias, Instituto de Estudios Avanzados IDEA, Caracas, Venezuela*
[c] *Instituto de Biología Experimental, Facultad de Ciencias, Universidad Central de Venezuela, Aptdo. 47114, Caracas, Venezuela*

Received 22 December 2004, and in revised form 5 January 2005
Available online 21 January 2005

Abstract

Using site-directed mutagenesis, we have produced three calmodulin (CaM) mutants in which one or the two tyrosine residues of native CaM were substituted by phenylalanine. The three variants, denoted CaM(Y99F), CaM(Y138F), and CaM(Y99F/Y138F), were highly expressed in transformed *Escherichia coli* BL21(DE3)pLysS and purified in high yield. The three CaM mutants were able to activate the cyclic nucleotide phosphodiesterase and the plasma membrane Ca^{2+}-ATPase, and present the characteristic Ca^{2+}-induced electrophoretic mobility shift of native CaM. CaM(Y138F) and CaM(Y99F/Y138F), however, showed a slightly higher electrophoretic mobility than CaM(Y99F) or wild type CaM. The molar extinction coefficient of native CaM at 276 nm decreases 50% in CaM(Y99F) and CaM(Y138F), while the 276 nm peak disappears in CaM(Y99F/Y138F). Terbium fluorescence studies with the different CaM mutants indicate that Y99 (but not Y138) closely interacts with Ca^{2+} in the III Ca^{2+}-binding domain. The epidermal growth factor receptor (EGFR) and the non-receptor tyrosine kinase c-Src phosphorylate CaM(Y99F) and CaM(Y138F) at a lesser extent than wild type CaM, while they fail to phosphorylate CaM(Y99F/Y138F) as expected. All resulting phospho-(Y)CaM species present the characteristic Ca^{2+}-induced electrophoretic mobility shift observed in non-phosphorylated CaM. Quantitative analysis of the different phospho-(Y)CaM species suggests that the relative phosphorylation of Y99 and Y138 in wild type CaM by both the EGFR and c-Src is different than the respective phosphorylation of either Y99 in CaM(Y138F) or Y138 in CaM(Y99F).

Keywords: Calmodulin mutants; Calmodulin phosphorylation; c-Src; Epidermal growth factor receptor

Calmodulin is an ubiquitous Ca^{2+}-binding protein that decodes oscillations in the concentration of intracellular free Ca^{2+} by acting as a sensor of this divalent cation in eukaryotic cells, and hence regulating a myriad of cellular processes [1,2]. In addition, apocalmodulin could also recognise various protein targets exerting certain functional role [3]. Despite the occurrence of different types of posttranslational modifications in CaM,[2] it is

* Corresponding author. Fax: +58 212 903 5118.
E-mail address: gbenaim@reacciun.ve (G. Benaim).
[1] These authors contributed equally to this work.
[2] *Abbreviations used:* CaM, calmodulin; EGF, epidermal growth factor; EGFR, epidermal growth factor receptor; EGTA, [ethylenebis (oxyethylenenitrilo)]tetraacetic acid; Hepes, 4-(2-hydroxyethyl)-1-piperazineethanesulfonic acid; IPTG, isopropyl-1-thio-β-D-galactopiranoside; Jak2, Janus kinase 2; P-CaM, phosphorylated calmodulin; PCR, polymerase chain reaction; PMSF, phenylmethylsulfonyl fluoride; PTB, phosphotyrosine binding; PVDS, polyvinylidene difluoride; SDS–PAGE, polyacrylamide gel electrophoresis in the presence of sodium dodecyl sulfate; SH2, Src non-catalytic homology 2; Tris, tris(hydroxymethyl)-aminomethane.

1046-5928/$ - see front matter © 2005 Elsevier Inc. All rights reserved.
doi:10.1016/j.pep.2005.01.004

not yet clear whether or not these modifications could play a significant part in the regulation of CaM-mediated cellular functions in intact cells either acting in the absence or presence of Ca^{2+}.

Phosphorylation of CaM by diverse protein-serine/threonine and protein-tyrosine kinases has been shown to take place not only in vitro but in vivo, and the different P-CaM species produced by these enzymes present distinct biological activities when acting on multiple CaM-dependent systems (see [4] for a review). Tyrosine phosphorylation of CaM by distinct receptor protein-tyrosine kinases, such as the insulin receptor [5,6] and the EGFR [7,8], and non-receptor kinases, such as different Src family kinases [9,10], Jak2 [11], and p38Syk [10], has been described. It is clear, therefore, that tyrosine-phosphorylation of CaM is a widespread phenomenon.

The P-(Y)CaM species generated by each of the above-mentioned protein-tyrosine kinases appear to be distinct as the phosphorylation stoichiometry of Y99 and Y138 varies depending on the kinase involved [4]. Although very little is known about the actual identity of the phosphoserine/threonine- and phosphotyrosine-protein phosphatases implicated in the dephosphorylation of P-CaM, firmly established observations on phosphorylation of CaM and the need for the reversibility of this process suggest that this posttranslational modification may play a prominent role in the modulation of the distinct physiological actions on which this Ca^{2+}-binding protein is involved. This modulation may occur in addition and/or instead of the canonical regulation mediated by changes in the concentration of intracellular free Ca^{2+} [4].

Mammalian CaM contains two single tyrosine residues at positions 99 and 138 [1]. Therefore, the availability of CaM mutants lacking either one or both tyrosine residues could be helpful tools to elucidate the potential involvement of each phosphorylated tyrosine residue of CaM on the functionality of target proteins. We describe in this work the characterisation of three CaM mutants bearing tyrosine to phenylalanine substitutions denoted CaM(Y99F), CaM(Y138F), and CaM(Y99F/Y138F), and therefore defective in tyrosine phosphorylation as shown using two protein-tyrosine kinases, the EGFR and c-Src. The results show interesting differences among the mutants, which represent new tools for the characterisation of CaM itself and for its interaction with target proteins.

Experimental procedures

Reagents

Radiolabelled [γ-^{32}P]ATP (triethylammonium salt) (3000 Ci mmol^{-1}) (1 Ci = 37 GBq), Hyperfilm-MP X-ray films and the ECL kit were purchased from Amersham–Pharmacia. Recombinant EGF (human) was obtained from PeproTech. The QuickChange site mutagenesis kit was from Stratagene, and the QIAprep plasmid preparation kit was obtained from Qiagen. Restriction enzymes were provided by Promega. Phosphodiesterase 3′:5′-cyclic nucleotide (from porcine brain), 5′-nucleotidase (from *Crotalus adamanteus* venom), phenyl–Sepharose CL-4B, calmodulin–agarose, Fast Green FCF, PMSF, ATP (sodium salt), cAMP (sodium salt), Triton X-100, Tween 20, histone (type II-AS from calf thymus, fractions containing histone H2, H3, and H4 as observed in SDS–PAGE), Hepes, and anti-mouse IgG (Fc specific) peroxidase-conjugated were obtained from Sigma. Monoclonal anti-phosphotyrosine antibody (4G10) and recombinant c-Src (human) were obtained from Upstate Biotechnology. PVDF membranes of 0.45 μm pore size (Immobilon-P) were from Millipore and thrombin (bovine) was from Calbiochem. Bovine brain calmodulin was purified essentially as described [12]. *Escherichia coli* cultures transformed with the pETCM vector was a kind gift of Prof. Nobuhiro Hayashi from Fujita Health University, Aichi, Japan. Other chemicals used in this work were of analytical grade.

Site-directed mutagenesis

PCR-aided site-directed mutagenesis was performed on the pETCM vector that contains the coding sequence from rat CaM [13] using the QuickChange site-directed mutagenesis kit and two sets of complementary oligos: 5′-GCTCTGCTGCACTGATGAAGCCATTGCCATCC-3′ and 5′-GGATGGCAATGGCTTCATCAGTGCAGCAGAGC-3′ for the Y99F substitution, and 5′-GGGGATGGTCAGGTAAACTTCGAAGAGTTTGTACAAATG-3′ and 5′-CATTTGTACAAACTCTTCGAAGTTTACCTGACCATCCCC-3′ for the Y138F substitution. Sequential mutagenesis was carried out to obtain the double substitution Y99F/Y138F. *E. coli* XL1-Blue was transformed with the modified vectors pETCM(Y99F), pETCM(Y138F), and pETCM(Y99F/Y138F), the plasmids were isolated by the alkaline lysis method [14] using the QIAprep plasmid preparation kit, and the correctness of the mutagenesis procedures was ascertained by direct sequencing the vectors using an oligo annealing to the T7 polymerase promoter.

Expression and purification of recombinant calmodulin

Escherichia coli BL21(DE3)pLysS was transformed with the pETCM, pETCM(Y99F), pETCM(Y138F), and pETCM(Y99F/Y138F) vectors, and wild type CaM and the three variants CaM(Y99F), CaM(Y138F), and CaM(Y99F/Y138F) were induced with 1 mM IPTG during 3 h in 800 ml of Luria–Bertani's broth supplemented with 100 μg/ml ampicillin and 34 μg/ml chloramphenicol. The different recombinant CaM species were purified as

described in [13], except that the soluble bacterial cell extract was heated at 95 °C for 5 min before the heat-resistant proteins remaining in the supernatant were subjected to phenyl–Sepharose chromatography [15].

Isolation of the EGF receptor

Taking advantage that the EGFR is a CaM-binding protein [7,15–17], an enriched fraction containing this receptor was isolated by Ca^{2+}-dependent CaM-affinity chromatography as previously described [7].

Phosphorylation assays

Unless indicated otherwise, phosphorylation of the different CaM species by the EGFR was carried out at 37 °C for 2 min in a total volume of 100 μl in a medium containing 15 mM Hepes–NaOH (pH 7.4), 5 mM $MgCl_2$, 0.4 mM EGTA, 2% (w/v) glycerol, 0.4% (w/v) Triton X-100, 1 μM EGF (when added), 120 μg/ml histone, 20 μg/ml CaM (histone:CaM molar ratio = 5), 10 μM (2 μCi) [γ-^{32}P]ATP, and 40 μl of the EGFR preparation. Phosphorylation assays using c-Src instead of the EGFR were carried out at 37 °C for 30 min in a total volume of 100 μl in a medium containing 15 mM Hepes–NaOH (pH 7.4), 5 mM $MgCl_2$, 1 mM EGTA, 1 mM dithiothreitol, 24 μg/ml histone, 20 μg/ml CaM (histone:CaM molar ratio = 1), 10 μM (2 μCi) [γ-^{32}P]ATP, and 2 U c-Src. One unit of c-Src transfers 6.2 pmol phosphate/min to its substrate peptide at 30 °C and pH 7.2. When Western blots using the anti-phosphotyrosine antibody were performed, the assays with either of the two protein-tyrosine kinases were carried out for 15–30 min using 2 mM non-radiolabelled ATP instead of [γ-^{32}P]ATP. The phosphorylation reaction was initiated upon addition of ATP and stopped with ice-cold 10% (w/v) trichloroacetic acid. The precipitated proteins were processed by SDS–PAGE and autoradiography as described below. The intensity of the bands present in the X-ray films were quantified by a computer-assisted scanner using the ScanImage program. Alternatively, when the resulting P-CaM species were destined for purification by phenyl–Sepharose chromatography, the assay mixture was scaled up by a factor of four, the trichloroacetic acid precipitation step was omitted, and the sample was rapidly ice-cooled before chromatographic processing.

Immunoblot analysis

Proteins separated by SDS–PAGE as described below were electrotransferred to a PVDF membrane at 300 mA for 2 h in a buffer containing 48 mM Tris (base) and 39 mM glycine (pH 8.3), 1.3 mM sodium dodecyl sulfate, and 20% (v/v) methanol. Proteins were fixed for 45 min with 0.2% (v/v) glutaraldehyde in TBS (25 mM Tris–HCl at pH 8, 150 mM NaCl, and 2.7 mM KCl) and transiently stained with 0.1% (w/v) Fast Green FCF in 50% (v/v) methanol and 10% (v/v) acetic acid. Thereafter, the membrane was blocked with 5% (w/v) bovine serum albumin in TBS for 2 h at room temperature, washed extensively with 0.1% (v/v) Tween 20 in TBS (TTBS), probed overnight with the anti-phosphotyrosine monoclonal antibody (4G10) at a 1:250 dilution, and an anti-mouse IgG conjugated to horseradish peroxidase at a 1:4000 dilution. Positive bands were detected using the enhanced chemiluminescence Luminol (ECL) method following instructions from the manufacturer.

Phosphodiesterase assay

The porcine brain CaM-dependent cyclic nucleotide phosphodiesterase activity was assayed at 37 °C for 15 min using 2.5 mM cAMP as substrate and the different CaM species (8 μg/ml) in the absence and presence of 0.1 mM free Ca^{2+} as previously described [18].

Plasma membrane Ca^{2+}-ATPase assay

Plasma membranes from human erythrocytes (ghosts) devoid of calmodulin were obtained as described [19]. The Ca^{2+}-ATPase activity was determined as previously described [20]. Briefly, aliquots of erythrocytes ghost (about 1–2 mg protein/ml) were incubated in a medium containing 130 mM KCl, 20 mM Hepes/KOH (pH 7.4), 1 mM $MgCl_2$, 1 mM ATP, 1 mM EGTA, and 1 mM $CaCl_2$, to obtain 10 μM free Ca^{2+} concentration. The reaction was carried out for 45-min incubation at 37 °C and was arrested by the addition of cold trichloroacetic acid at 8% (w/v). The mixture was centrifuged and the supernatant was kept for inorganic phosphate determination. The phosphate produced by ATP hydrolysis was determined as previously described [21], modified by the use of $FeSO_4$ as the reducing agent.

Fluorescence measurements

Different CaM species were assayed at 10 μM final concentration in a buffer containing 10 mM Pipes (pH 6.5), 100 mM KCl, and different concentrations of $TbCl_3$. The fluorescence of tyrosines was measured in a fluorimeter (Perkin-Elmer LS50), using 280 and 307 nm as excitation and emission wavelength, respectively [22].

Isolation of phosphocalmodulin and thrombinisation assay

The different P-CaM species were purified by Ca^{2+}-dependent hydrophobic-interaction chromatography as follows: the 4-fold scaled up phosphorylation assay mixture described above using [γ-^{32}P]ATP as substrate was ice-cooled after the reaction was completed and diluted to 1.5 ml with a buffer containing 50 mM Hepes–NaOH (pH 7.4), 50 mM NaCl, and 0.1 mM $CaCl_2$ (Ca-buffer A).

The sample was adjusted to 0.1 mM free Ca^{2+} using additional $CaCl_2$ and immediately passed through a 1 ml phenyl-Sepharose column equilibrated with Ca-buffer A. The column was extensively washed, first with 40 ml of a modified Ca-buffer containing 0.5 M NaCl (Ca-buffer B), and thereafter with 40 ml of Ca-buffer A. The phosphorylated and non-phosphorylated forms of CaM were eluted in 0.4 ml fractions using a modified buffer A containing 1 mM EGTA instead of $CaCl_2$ (EGTA-buffer). The purified P-CaM species were incubated with 2.5 U thrombin for 3–15 min at 37 °C in a buffer containing 50 mM Hepes–NaOH (pH 7.4), 50 mM NaCl, and 1 mM EGTA. One unit of thrombin was defined by comparison to a thrombin standard prepared by the Bureau of Biologic Standards as mentioned by the manufacturer.

Other analytical procedures

Slab gel electrophoresis was performed as described in [23] at 12 mA overnight in a 5–20% (w/v) polyacrylamide linear gradient gel or at 60 mA for 3 h in a 12% (w/v) polyacrylamide gel, both in the presence of 0.1% (w/v) sodium dodecyl sulfate at pH 8.3. To attain the characteristic Ca^{2+}-induced electrophoretic mobility shift of CaM [24], we added either 5 mM EGTA or 5 mM $CaCl_2$ to the electrophoresis loading buffer. Gels were stained with Coomassie Brilliant Blue R-250, dried under vacuum at 80 °C for 2 h on Whatman 3MM Chr filter paper, and when required blue-sensitive X-ray films were exposed at −20 °C for 1–3 days to obtain autoradiographies. The protein concentration was determined as described [25] after precipitation of proteins with 10% (w/v) trichloroacetic acid and using bovine serum albumin as a standard.

Results

Characterisation of tyrosine–calmodulin mutants

Site-directed mutagenesis consisting in the modification of one or two TAC codons for TTC codons in the coding sequence for rat CaM were performed on the pETCM vector resulting in the substitution of either one or the two tyrosine residues of native CaM for phenylalanine, yielding three CaM mutants denoted CaM (Y99F), CaM(Y138F), and CaM(Y99F/Y138F).

The expression level of wild type CaM and the three CaM variants in *E. coli* BL21(DE3)pLysS transformed with the pETCM, pETCM(Y99F), pETCM(Y138F), and pETCM(Y99F/Y138F) vectors, and induced by IPTG were very similar as shown in Fig. 1. The four recombinant CaM variants were purified to homogeneity in high yield by Ca^{2+}-dependent hydrophobic-interaction chromatography modified as previously described [13,15]. We obtained an average ± SEM purification yield and recovery as follows: from 331 ± 30 mg ($n = 3$) total protein from the bacterial extract we obtained 99 ± 14 mg ($n = 4$) soluble protein after heating at 95 °C for 5 min (30 ± 4% recovery), and 35 ± 4 mg ($n = 4$) purified CaM (11 ± 1% recovery) after phenyl-Sepharose chromatography.

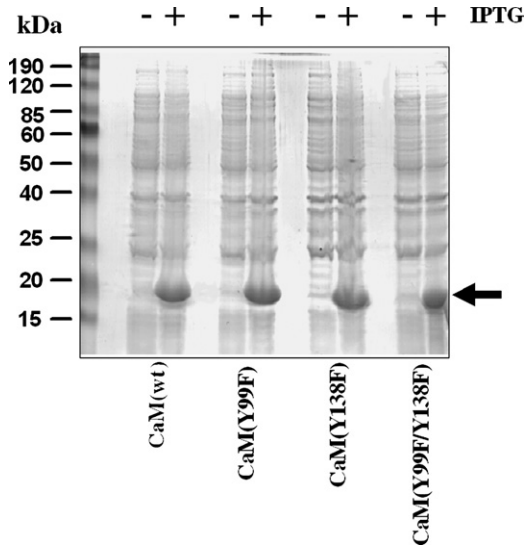

Fig. 1. Expression of recombinant CaM mutants. Total cell extracts from an identical volume (12 µl) of *E. coli* BL21(DE3)pLysS cultures transformed with the different CaM expression vectors and incubated in the absence (−) and presence (+) of 1 mM IPTG were resolved by 12% SDS–PAGE in the presence of 5 mM EGTA and stained with Coomassie blue as described under Experimental procedures. The arrow points to the different recombinant CaM species.

Fig. 2 shows that the three purified CaM mutants were homogeneous as observed in SDS–PAGE carried out in the presence of EGTA, and present the characteristic Ca^{2+}-induced electrophoretic mobility shift observed in wild type CaM [24]. The double band

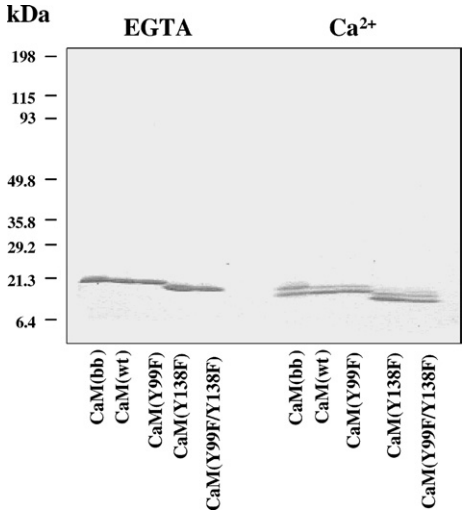

Fig. 2. Electrophoretic mobility of CaM mutants. The different purified recombinant CaM species, and a control of bovine brain (bb) CaM (2 µg) were processed by 5–20% SDS–PAGE in the presence of 5 mM EGTA or 5 mM $CaCl_2$ as indicated, and stained with Coomassie blue as described under Experimental procedures.

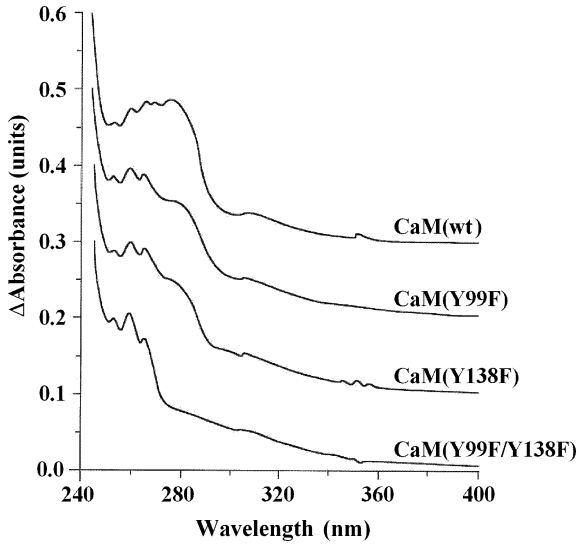

Fig. 3. Absorption spectra of CaM mutants. The UV-light absorption spectra were recorded in a Shimadzu UV-160A spectrophotometer using a 1 mg/ml solution of the different recombinant CaM species purified as described under Experimental procedures and dialysed against 10 mM Hepes–NaOH (pH 7.4). For clarity, the spectra are arbitrarily plotted setting the base lines at different absorbance values to avoid superimposition.

noticed in the presence of Ca^{2+} is a well-documented observation, and could represent the differential electrophoretic migration of diverse Ca^{2+}–CaM complexes with variable Ca^{2+} binding stoichiometry. Nevertheless, CaM(Y138F) and CaM(Y99F/Y138F) show a slightly higher electrophoretic mobility than that of CaM(Y99F), recombinant wild type CaM, or bovine brain CaM, both in the absence or presence of Ca^{2+}.

The UV-light absorption spectrum of wild type CaM reveals a prominent peak at 276 nm which is mostly due to the presence of tyrosine residues [26]. Thus, and as expected, Fig. 3 shows that both CaM(Y99F) and CaM(Y138F) present a significant reduction in absorbance at 276 nm, and CaM(Y99F/Y138F) totally lacks this 276 nm peak. Wild type CaM has an $E_{M,\ 276\,nm} = 3740$ [26]. However, taking into consideration the progressive decline in the photon efficiency at shorter wavelength, CaM(Y99F) and CaM(Y138F) both present a 50% reduction in its $E_{M,\ 276\,nm}$, and CaM(Y99F/Y138F) has an $E_{M,\ 276\,nm}$ close to zero.

We also performed experiments to study the interaction of Tb^{3+} with the Ca^{2+}-binding domains of the different mutants, taking advantage of the fact that Y99 and Y138 form part of the aminoacidic sequence involved in the Ca^{2+}-binding domains III and IV, respectively. Thus, we measured the fluorescence of tyrosine residues, using Tb^{3+} as a surrogate for Ca^{2+} [22], exciting at 280 nm while registering at 307 nm as emission wavelength. The results are presented as the relative fluorescence quenching of tyrosine residues induced by Tb^{3+}.

Fig. 4 shows a Tb^{3+} concentration dependent increase in tyrosine fluorescence quenching when wild type CaM and CaM(Y138F) were used, while both CaM variants modified in Y99 failed to show a significant change over the whole range of Tb^{3+} concentrations assayed. These results indicated that Tb^{3+} is closer to Y99 than to Y138 producing, therefore, fluorescence quenching.

To analyse the effect of the performed tyrosine to phenylalanine substitutions on the biological activity of CaM, we tested the capacity of the different CaM mutants to activate a CaM-dependent cyclic nucleotide phosphodiesterase using cAMP as substrate [27]. Fig. 5A shows that indeed this is the case as CaM(Y99F), CaM(Y138F), and CaM(Y99F/Y138F) at a saturating concentration stimulated the activity of this enzyme in the presence of Ca^{2+} (filled bars) to essentially the same level than recombinant wild type CaM or bovine brain CaM. No significant variance was also found in the basal activity of the enzyme measured with the different CaM species in the absence of Ca^{2+} (empty bars). We also tested the ability of the different CaM mutants to stimulate the plasma membrane Ca^{2+}-ATPase from human erythrocytes. As can be seen in Fig. 5B, all CaM variants are able to stimulate the Ca^{2+}-ATPase activity. Unexpectedly, the double mutant CaM(Y99F/Y138F) was more effective stimulating the Ca^{2+}-ATPase activity than wild type CaM since a small but significant increase in the V_{max} of the enzyme was detected.

Phosphorylation of tyrosine–calmodulin mutants

To determine the effect of the different mutations on the phosphorylation of CaM by protein-tyrosine kinases, we assayed the CaM mutants with the EGFR and c-Src. Fig. 6A shows that the EGFR in the presence of EGF is able to phosphorylate CaM(Y99F) (lanes 3) and CaM(Y138F) (lanes 4) but fails to phosphorylate CaM(Y99F/Y138F) (lanes 5) as expected. Controls

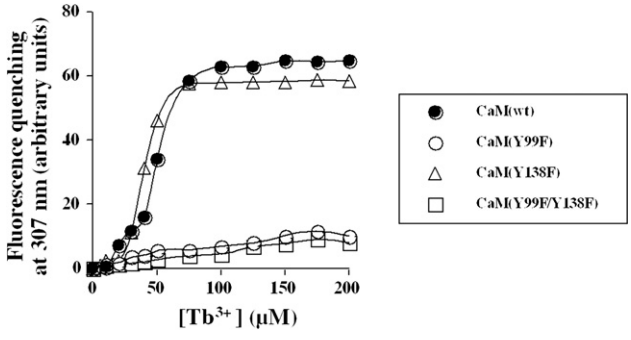

Fig. 4. Tb^3-induced quenching of tyrosine fluorescence in CaM mutants. The results are presented as the fractional quenching of tyrosine fluorescence induced by different concentrations of Tb^{3+} using the different CaM species determined as described under Experimental procedures. The concentration of the different CaM species was 10 μM.

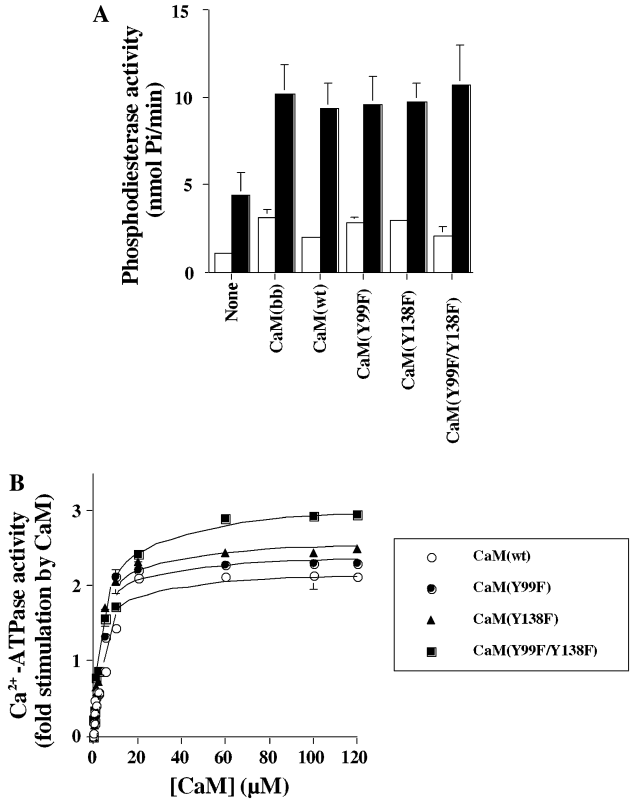

Fig. 5. Activation of CaM-dependent enzymes by CaM mutants. (A) The cyclic nucleotide phosphodiesterase activity was assayed in the absence and presence of the different recombinant CaM species or bovine brain (bb) CaM (8 μg/ml) in the absence (empty bars) and presence (filled bars) of Ca^{2+} as described under Experimental procedures. The average ± SEM of duplicated samples in two separate experiments are shown. (B) The Ca^{2+}-ATPase was assayed at different concentrations of wild type and CaM mutants in the presence of 10 μM free Ca^{2+} as described under Experimental procedures. The average ± SEM of triplicate samples from three separate experiments are shown.

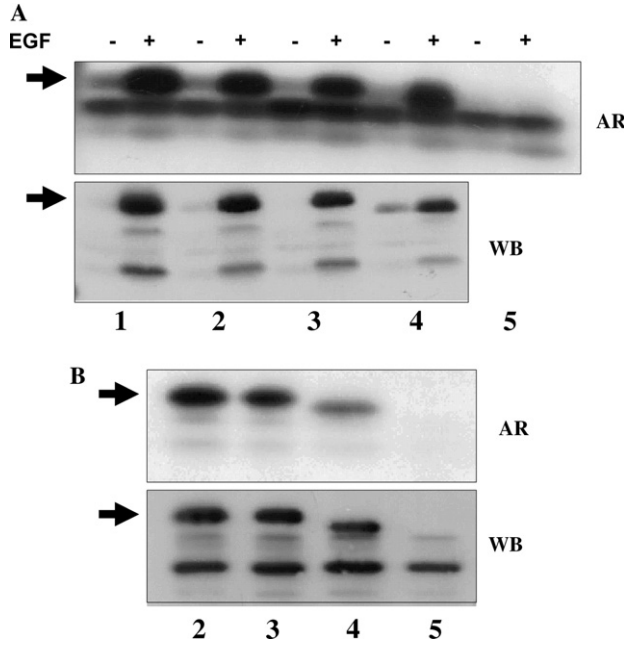

Fig. 6. Phosphorylation of CaM mutants by the EGFR and c-Src. Bovine brain CaM (lanes 1), recombinant wild type CaM (lanes 2), CaM(Y99F) (lanes 3), CaM(Y138F) (lanes 4), and CaM(Y99F/Y138F) (lanes 5) were phosphorylated by the EGFR (A) in the absence (−) and presence (+) of EGF, or by c-Src (B) using the radioactive (AR panel) or non-radioactive (WB panel) assay systems as described under Experimental procedures, and processed in 5–20% SDS–PAGE in the presence of 5 mM EGTA. The radioactive assays contained 2 μg CaM, and the non-radioactive assays contained 2.5 or 3 μg CaM, respectively, when the EGFR and c-Src were used. Histone/CaM (mol/mol) ratios of 5 for the EGFR assays, and 1 for the c-Src assays were used. The arrow points to P-CaM.

using bovine brain CaM (lanes 1) and recombinant wild type CaM (lanes 2) are also shown. Only trace phosphorylation in the absence of EGF was detected. Similar results were obtained in assays using either [γ-^{32}P]ATP developed by autoradiography (AR panel) or non-radiolabelled ATP developed by Western blot using an anti-phosphotyrosine antibody (WB panel). Additional experiments using non-radiolabelled ATP and the Western blot assay system demonstrated that phosphorylation of CaM(Y99F/Y138F) gave a negative signal as expected (not shown). Densitometric analysis of different experiments shows that the average phosphorylation of CaM(Y99F) and CaM(Y138F) by the EGFR was, respectively, 68 ± 11% and 68 ± 5% as compared to the phosphorylation of recombinant wild type CaM.

Fig. 6B shows that phosphorylation of the CaM mutants by c-Src gave similar results to those obtained with the EGFR using the radioactive (AR panel) or the non-radioactive (WB panel) assay systems. Quantitative analysis of different experiments reveals that the average ± SEM phosphorylation of the two single-tyrosine CaM mutants by c-Src was 74 ± 7% ($n = 3$) for CaM(Y99F) and 52 ± 10% ($n = 3$) for CaM(Y138F) as compared to the phosphorylation of recombinant wild type CaM.

We have also determined in Fig. 7 that the phosphorylated forms of recombinant wild type CaM (lanes 1), CaM(Y99F) (lanes 2), and CaM(Y138F) (lanes 3) as phosphorylated by the EGFR (A) and c-Src (B) present the characteristic Ca^{2+}-induced electrophoretic mobility shift observed in their non-phosphorylated counterparts (see Fig. 2) when processed in the presence of EGTA or $CaCl_2$ as indicated.

Thrombin cleaves CaM in the absence of Ca^{2+} at a single site (R106-H107), located between the third and fourth Ca^{2+}-binding sites, yielding a large fragment containing Y99, and a smaller fragment containing Y138 [28,29]. Taking advantage of this fact, we performed thrombinisation assays with recombinant wild type P-CaM, P-CaM(Y99F), and P-CaM(Y138F) purified by phenyl-Sepharose chromatography and phosphorylated by c-Src to further characterise these CaM mutants. Fig. 8 shows that purified wild type P-CaM (lanes 1)

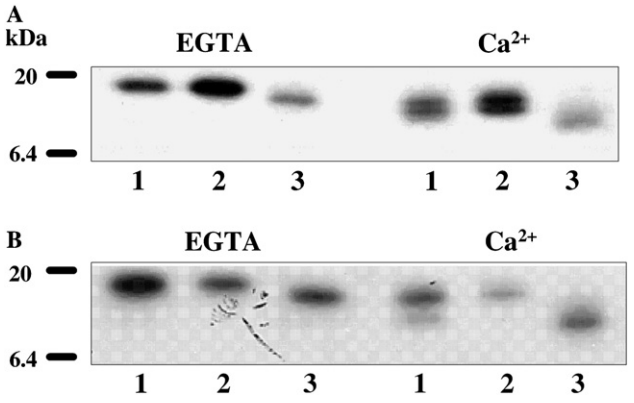

Fig. 7. Electrophoretic mobility of P-CaM mutants. Recombinant wild type CaM (lanes 1), CaM(Y99F) (lanes 2), and CaM(Y138F) (lanes 3) were phosphorylated by the EGFR (A) and c-Src (B), and thereafter purified as described under Experimental procedures. Samples containing approximately 1–2 μg CaM were processed by 5–20% SDS–PAGE in the presence of 5 mM EGTA or 5 mM $CaCl_2$ as indicated.

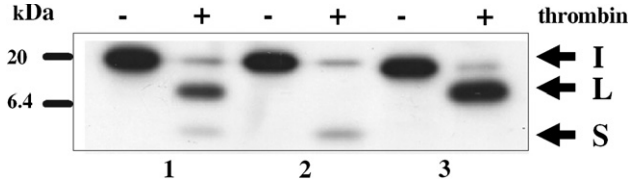

Fig. 8. Thrombinisation of P-CaM mutants. Recombinant wild type CaM (lane 1), CaM(Y99F) (lane 2), and CaM(Y138F) (lane 3) were phosphorylated by c-Src, purified by phenyl–Sepharose chromatography, and incubated in the absence (−) and presence (+) of 2.5 U thrombin in the presence of 1 mM EGTA as described under Experimental procedures. Samples containing approximately 1 μg CaM were processed by 5–20% SDS–PAGE in the presence of 5 mM EGTA. Intact P-CaM (I), and the large (L), and small (S) P-CaM fragments are indicated by arrows.

treated with thrombin in the presence of EGTA produces both phosphorylated fragments, showing that the large fragment (L) was more intensively labelled than the small fragment (S), while P-CaM(Y99F) (lane 2) and P-CaM(Y138) (lane 3) only yield, respectively, either the faintly labelled small fragment (S) or the more intensively labelled large fragment (L). A significant decrease in the labelling of the thrombin-treated samples was apparent, as the combined labelling of the two P-CaM fragments (L and S) plus the residual non-thrombinised P-CaM band (I) was lower than the labelling of the control P-CaM in non-treated samples.

Discussion

The three recombinant tyrosine-deficient CaM mutants described in this report show the expected behaviour in regard to their similar expression levels in bacteria, and most of the tested physico-chemical properties. Thus, the decrease in absorbance at 276 nm, a characteristic absorption peak of wild type CaM [26], as observed on their UV-light absorption spectra, and the maintenance of the Ca^{2+}-induced electrophoretic mobility shift typical of native CaM [24] are conspicuous features. Moreover, the three CaM variants conserve their biological activity, as they retain the capacity to activate classical CaM-dependent enzymes, such as the cyclic nucleotide phosphodiesterase [27] and the plasma membrane Ca^{2+}-ATPase [30,31]. It was interesting to observe that the double mutant CaM(Y99F/Y138F) was slightly more potent stimulating the Ca^{2+}-ATPase activity than wild type CaM. Other authors have shown that a poorly characterised chicken CaM mutant with a Y138F substitution has lower affinity for the Ca^{2+}-ATPase than native CaM [32].

Concerning the quenching of tyrosine fluorescence induced by Tb^{3+} in wild type CaM and in CaM(Y138F), the easiest explanation is that Y99 in the III Ca^{2+}-binding pocket is close enough to Tb^{3+} to absorb the tyrosine-emitted fluorescence, while Y138 in the IV Ca^{2+}-binding pocket is not. Indeed it has been shown by X-ray crystallography that the carbonyl group of Y99 contributes directly to the conjugation of Ca^{2+}, forming one of the vertices of the Ca^{2+} octahedron in the E–F hand, while Y138, albeit being in the aminoacidic sequence which forms the IV Ca^{2+}-binding pocket, does not contribute directly to Ca^{2+} conjugation.

We have noticed other differences in some properties between wild type CaM and the described CaM mutants which are worthwhile to mention. The most remarkable one is the Ca^{2+}-independent increase in electrophoretic mobility observed in CaM(Y138F) and CaM(Y99F/Y138F) as compared to wild type CaM or CaM(Y99F). We believe that it is quite unlikely that the absence of the -OH group of one or two tyrosine residues could significantly change the net ionisation of CaM to explain the observed difference in electrophoretic migration among the different CaM species. Hence, since CaM retains certain degree of its native conformation in denaturalising SDS–PAGE [24], we suggest that the Y138F substitution, but not the Y99F substitution, somewhat affects the overall tridimensional structure of CaM. Up to date, the reason for the faster migration of CaM in the presence of Ca^{2+} is not known. However, there are two possible explanations: (i) that CaM in the presence of Ca^{2+} adopts a more compact form generating less friction during its migration through the gel; and (ii) the protein could bind more SDS per mol presenting more negative charges of the complex to be attracted to the anode since the binding of Ca^{2+} to CaM is known to induce an increase in its α-helix content and to expose more hydrophobic residues. In this context, it is apparent that the Y138F substitution induces either a larger condensation of the molecule or a higher degree of hydrophobicity which is transduced in a faster migration.

Interestingly, the two single-tyrosine mutants, CaM(Y99F) and CaM(Y138F), were phosphorylated by the EGFR to an extent somewhat higher than the 50%

expected if Y99 and Y138 in each mutant were equally phosphorylated at half the extent than in wild type CaM. In contrast, CaM(Y99F), but not CaM(Y138F), was phosphorylate by c-Src to values higher than 50% of the phosphorylation observed in wild type CaM. These overall measurements suggest that phosphorylation of Y138 in CaM(Y99F) occurs at a higher or equal extent than the phosphorylation of Y99 in CaM(Y138F). These results are at odd with the reported preferential phosphorylation of Y99 as compared to Y138 in wild type CaM using the insulin receptor, the EGFR, c-Src, and other Src family kinases [4]. Thus, we propose that a mutation at a single tyrosine residue of CaM somewhat alters the phosphorylation extent of the remaining tyrosine residue. Therefore, each species of CaM behaves differently as protein-tyrosine kinase substrate, most likely because the presentation of each tyrosine residue to the catalytic site of the different protein-tyrosine kinases varies, in agreement with the suggested change in conformation of these mutants based on their dissimilar electrophoretic mobility as described above.

Thrombin is a serine-protease involved in multiple physiological functions [33]. Beside its well-known action in hemostasis converting fibrinogen into fibrin, and activating diverse coagulation factors, it activates platelets and other cell types by binding, proteolysing and hence activating protease-activated receptors 1–4 (PAR1–4). PAR1–4 are G protein-coupled receptors whose signals result in cell proliferation, extracellular matrix production, and induction of an inflammatory response among others. Thrombinisation of CaM in the presence of EGTA occurs between R106 and H107, yielding two distinct fragments each containing a single tyrosine residue, Y99 in the large fragment and Y138 in the small fragment [28,29]. In the presence of Ca^{2+}, however, proteolysis at the R106–H107 site significantly decreases and a new proteolytic site located between R37 and S38 [29] comes into view. This protease has been used, therefore, to establish the phosphorylation stoichiometry of Y99 and Y138 in wild type CaM in assays performed in the absence of Ca^{2+} by determining the relative amount of [^{32}P]phosphate bound to the two thrombin-generated fragments of CaM [4]. Taking into consideration these observations, we have compared the thrombinisation fingerprint of purified wild type P-CaM, P-CaM(Y99F), and P-CaM(Y138F) as phosphorylated by c-Src, measuring the relative intensity of the two ^{32}P-labelled fragments. We have determined that the small fragment from P-CaM(Y99F), containing phosphorylated Y138, was more weakly labelled than the large fragment from P-CaM(Y138F), containing phosphorylated Y99, in agreement with the thrombinisation pattern observed in wild type P-CaM. Nevertheless, as we have indicated above, the phosphorylation of CaM(Y138F) by c-Src was less intense that the phosphorylation of CaM(Y99F) using the same kinase. We have as well noticed that the thrombin-produced ^{32}P-labelled fragments from P-CaM do not maintain the same amount of label than the non-treated samples. This is particularly clear for the small fragment. Two processes could account for this observation: (i) a differential dephosphorylation of both ^{32}P-labelled fragments, and/or (ii) the existence of unnoticed additional proteolytic events of both fragments yielding very small ^{32}P-labelled peptides which could be lost on the electrophoretic front. We suggest, therefore, that the thrombinisation assay may not be a reliable method to measure the real phosphorylation levels of both tyrosine residues in P-CaM, and therefore invalid to determine their relative phosphorylation stoichiometries.

Although CaM and different P-(Y)CaM species have been shown to differentially modulate some CaM-dependent target proteins in vitro [4], more detailed analysis using additional CaM-dependent systems is needed. Likewise, the potential physiological role of the two phosphorylated tyrosine residues of wild type CaM has not been established in intact cells. We believe that the described CaM mutants could be useful tools to answer these questions, as the role of each phosphorylated tyrosine residue can be assessed in a variety of CaM-dependent enzymes not only in vitro, but also in vivo, using stable transfected cells overexpressing these CaM mutants, and/or using transfectants expressing these CaM variants as dominant-negative mutants. Moreover, further work should be performed to establish whether different P-(Y)CaM species could be used as bait to isolate specific signalling proteins containing SH2 and/or PTB domains to determine their potential role on CaM-dependent pathways.

Acknowledgments

This work was supported by grants from the *Comisión Interministerial de Ciencia y Tecnología* (SAF2002-03258), the *Consejería de Educación y Cultura de la Comunidad de Madrid* (08.1/0027/2001-1), and the *Agencia Española de Cooperación Internacional* (2002CN0013) to A.V., grants from the *Fondo Nacional para la Ciencia y Tecnología*, Venezuela (S1-1999000058 and G-2001000637) and from the *Consejo de Desarrollo Científico y Humanístico de la Universidad Central de Venezuela* (PI-03-10-4798-01) to G.B., and grant from the Spanish Ministry of Education (*Programa de Cooperación con Iberoamérica* to A.V. and G.B). V.S. was supported by a predoctoral fellowship from the *Consejo de Desarrollo Científico y Humanístico de la Universidad Central de Venezuela*.

References

[1] C.B. Klee, T.C. Vanaman, Calmodulin, Adv. Prot. Chem. 35 (1982) 213–321.
[2] D. Chin, A.R. Means, Calmodulin: a prototypical calcium sensor, Trends Cell Biol. 10 (2000) 322–328.

[3] L.A. Jurado, P.S. Chockalingam, H.W. Jarrett, Apocalmodulin, Physiol. Rev. 79 (1999) 661–682.
[4] G. Benaim, A. Villalobo, Phosphorylation of calmodulin: functional implications, Eur. J. Biochem. 269 (2002) 3619–3631.
[5] H.U. Haring, M.F. White, C.R. Kahn, Z. Ahmad, A.A. DePaoli-Roach, P.J. Roach, Interaction of the insulin receptor kinase with serine/threonine kinases in vitro, J. Cell. Biochem. 28 (1985) 171–182.
[6] C.B. Graves, R.D. Gale, J.P. Laurino, J.M. McDonald, The insulin receptor and calmodulin: calmodulin enhances insulin-mediated receptor kinase activity and insulin stimulates phosphorylation of calmodulin, J. Biol. Chem. 261 (1986) 10429–10438.
[7] E. San José, A. Benguría, P. Geller, A. Villalobo, Calmodulin inhibits the epidermal growth factor receptor tyrosine kinase, J. Biol. Chem. 267 (1992) 15237–15245.
[8] A. Benguría, O. Hernández-Perera, M.T. Martínez-Pastor, D.B. Sacks, A. Villalobo, Phosphorylation of calmodulin by the epidermal-growth-factor-receptor tyrosine kinase, Eur. J. Biochem. 224 (1994) 909–916.
[9] Y. Fukami, T. Nakamura, A. Nakayama, T. Kanehisa, Phosphorylation of tyrosine residues of calmodulin in *Rous sarcoma* virus-transformed cells, Proc. Natl. Acad. Sci. USA 83 (1986) 4190–4193.
[10] F. Meggio, A.M. Brunati, L.A. Pinna, Polycation-dependent, Ca^{2+}-antagonized phosphorylation of calmodulin by casein kinase-2 and spleen tyrosine protein kinase, FEBS Lett. 215 (1987) 241–246.
[11] Y.V. Mukhin, T. Vlasova, A.A. Jaffa, G. Collinsworth, J.L. Bell, B.G. Tholanikunnel, T. Pettus, W. Fitzgibbon, D.W. Ploth, J.R. Raymond, M.N. Garnovskaya, Bradykinin B_2 receptors activate Na^+/H^+ exchange in mIMCD-3 cells via Janus kinase 2 and Ca^{2+}/calmodulin, J. Biol. Chem. 276 (2001) 17339–17346.
[12] J.R Dedman, M.A. Kaetzel, Calmodulin purification and fluorescent labelling, Methods Enzymol. 102 (1983) 1–8.
[13] N. Hayashi, M. Matsubara, A. Takasaki, K. Titani, H. Taniguchi, An expression system of rat calmodulin using T17 phage promoter in *Escherichia coli*, Prot. Express. Purif. 12 (1998) 25–28.
[14] H.C. Birnboim, J.A. Doly, A rapid alkaline lysis procedure for screening recombinant plasmid DNA, Nucleic Acids Res. 7 (1979) 1513–1522.
[15] H. Li, A. Villalobo, Evidence for the direct interaction between calmodulin and the human epidermal growth factor receptor, Biochem. J. 362 (2002) 499–505.
[16] J. Martín-Nieto, A. Villalobo, The human epidermal growth factor receptor contains a juxtamembrane calmodulin-binding site, Biochemistry 37 (1998) 227–236.
[17] H. Li, M.J. Ruano, A. Villalobo, Endogenous calmodulin interacts with the epidermal growth factor receptor in living cells, FEBS Lett. 559 (2004) 175–180.
[18] P.I. Palomo-Jiménez, S. Hernández-Hernando, R.M. García-Nieto, A. Villalobo, A method for the purification of phospho(Tyr)calmodulin free of non-phosphorylated calmodulin, Prot. Express. Purif. 16 (1999) 388–395.
[19] G. Benaim, M. Zurini, E. Carafoli, Different conformational states of the purified Ca^{2+}-ATPase of the erythrocyte plasma membrane revealed by controlled trypsin proteolysis, J. Biol. Chem. 259 (1984) 8471–8477.
[20] C. Colina, V. Cervino, G. Benaim, Ceramide and sphingosine have an antagonistic effect on the plasma membrane Ca^{2+}-ATPase from human erythrocytes, Biochem. J. 362 (2002) 247–251.
[21] C.H. Fiske, Y. SubbaRow, The colorimetric determination of phosphorus, J. Biol. Chem. 66 (1925) 375–400.
[22] R.W Wallace, E.A. Tallant, M.E. Dockter, W.Y. Cheung, Calcium binding domains of calmodulin: sequence of fill as determined with terbium luminescence, J. Biol. Chem. 257 (1982) 1845–1854.
[23] U.K. Laemmli, Cleavage of structural proteins during the assembly of the head of bacteriophage T4, Nature 227 (1970) 680–685.
[24] W.H. Burgess, D.K. Jemiolo, R.H. Kretsinger, Interaction of calcium and calmodulin in the presence of sodium dodecyl sulfate, Biochim. Biophys. Acta 623 (1980) 257–270.
[25] O.H. Lowry, N.J. Rosebrough, A.L. Farr, R.J. Randall, Protein measurement with the Folin phenol reagent, J. Biol. Chem. 193 (1951) 265–275.
[26] D.J. Wolff, P.G. Poirier, C.A. Brostrom, M.A. Brostrom, Divalent cation binding properties of bovine brain Ca^{2+}-dependent regulator protein, J. Biol. Chem. 252 (1977) 4108–4117.
[27] R. Kakkar, R.V.S. Raju, R.K. Sharma, Calmodulin-dependent cyclic nucleotide phosphodiesterase (PDE1), Cell. Mol. Life Sci. 55 (1999) 1164–1186.
[28] C.M. Wall, R.J.A. Grand, S.V. Perry, Biological activities of the peptides obtained by digestion of troponin C and calmodulin with thrombin, Biochem. J. 195 (1981) 307–316.
[29] M.A. Shea, A.S. Verhoeven, S. Pedigo, Calcium-induced interactions of calmodulin domains revealed by quantitative thrombin footprinting of Arg37 and Arg106, Biochemistry 35 (1996) 2943–2957.
[30] R.M. Gopinath, F.F. Vincenzi, Phosphodiesterase protein activator mimics red blood cell cytoplasmic activator of the (Ca^{2+}–Mg^{2+})-ATPase, Biochem. Biophys. Res. Commun. 77 (1977) 1203–1209.
[31] H.W. Jarret, J.T. Penniston, Partial purification of the (Ca^{2+}–Mg^{2+})-ATPase activator from human erythrocytes: its similarity to the activator 3′–5′ cyclic nucleotide phosphodiesterase, Biochem. Biophys. Res. Commun. 77 (1977) 1210–1216.
[32] D.B. Sacks, M.M. Lopez, Z. Li, D. Kosk-Kosicka, Analysis of phosphorylation and mutation of tyrosine residues of calmodulin on its activation of the erythrocyte Ca^{2+}-transporting ATPase, Eur. J. Biochem. 239 (1996) 98–104.
[33] S.R. Coughlin, Thrombin signalling and protease-activated receptors, Nature 407 (2000) 258–264.